

# Diversity-Multiplexing Tradeoff for Multi-Connectivity and the Gain of Joint Decoding

Albrecht Wolf, Philipp Schulz, David Öhmann, *Member, IEEE*,  
Meik Dörpinghaus, *Member, IEEE*, and Gerhard Fettweis, *Fellow, IEEE*

## Abstract

Multi-connectivity (MC) is considered to be key for enabling ultra-reliable low latency communications in 5G. As MC architectures can realize an orthogonal multiple access channel (MAC) by using different carrier frequencies, the information can, in the best case, be delivered in a single time slot. The orthogonal MAC allows for a diversity gain, which can be exploited by different combining algorithms such as joint decoding (JD), maximum selection combining (MSC), and maximum ratio combining (MRC). We evaluate the outage probability of various MC setups and the different combining algorithms. For doing so, we establish a simple, yet accurate analytical framework where the number of links, the spectral efficiency, and the signal-to-noise ratios are incorporated. The main contributions are: 1) We find that JD requires less transmit power than MRC and MSC to achieve a given outage probability, assuming equal noise power. Interestingly, we find that JD becomes more advantageous with an increasing number of links as well as increasing spectral efficiency. 2) We derive the JD diversity-multiplexing tradeoff and show that JD can achieve both the maximum diversity gain and the maximum multiplexing gain for the MC setup. By contrast, MSC and MRC can merely achieve the maximum diversity gain.

## Index Terms

Diversity-multiplexing tradeoff, joint decoding, multi-connectivity, multiterminal source-channel coding, outage probability.

## I. INTRODUCTION

Fifth-generation mobile networks (5G) will face several challenges to cope with emerging application scenarios [3] in the context of ultra-reliable low latency communications (URLLC) such as mission critical industrial automation or communications for vehicular coordination which require an extremely high reliability (e.g., frame error rates of  $10^{-9}$ ) while simultaneously providing low latency (e.g., 1 ms end-to-end delay). These requirements pose a massive challenge on the physical layer. In fourth-generation mobile networks (4G), reliability is obtained by the hybrid automatic repeat request procedure, which retransmits erroneously received packets. However, the tight timing constraint of URLLC does not endorse multiple retransmissions.

Multi-connectivity (MC) is seen as a promising concept to enable URLLC in 5G [4] by establishing multiple diversity branches in the frequency domain. Different combining algorithms are known to take advantage of the multiple diversity branches. In this work, we concentrate on three combining algorithms which are joint decoding (JD), maximum selection combining (MSC), and maximum ratio combining (MRC), and derive the corresponding outage probabilities. We establish a remarkably simple, yet accurate analytical framework where the number of links, the spectral efficiency (associated with the code rate and the modulation scheme), and the received signal-to-noise ratio (SNR) are key parameters. By deriving the SNR gain and diversity-multiplexing tradeoffs (DMTs), we show that JD outperforms MSC and MRC. Next, we briefly describe MC, the combining algorithms, and then outline our approach and our contributions.

### A. Multi-Connectivity

In wireless communications, MC concepts have been mainly developed and applied for increasing data rates and capacity. Various ways exist to realize MC and we distinguish between two types, namely, intra- and inter-frequency MC. For instance, in case of intra-frequency MC in the downlink, multiple base stations (BSs) use the same carrier frequency to jointly transmit signals to a user. As a result, the received signal power and quality are improved, and diversity is facilitated. Established principles realizing intra-frequency MC are single frequency networks [5] and coordinated multi-point [6], [7]. Another type of MC is inter-frequency MC, where one or more BSs use multiple carrier frequencies to simultaneously transmit signals to a single user. In 4G, concepts such as carrier aggregation (CA) and dual connectivity (DC) have been introduced to make use

The material in this work has been accepted in part at the IEEE GLOBECOM, Singapore, Dec., 2017, [1], and will be submitted in part to the IEEE ICC, Kansas City, MO, USA, May, 2018 [2].

This work was supported in part by the Federal Ministry of Education and Research within the programme “Twenty20 - Partnership for Innovation” under contract 03ZZ0505B - “fast wireless”, in part by the German Research Foundation (DFG) within the SFB 912 “Highly Adaptive Energy-Efficient Computing (HAEC)”, and in part by the DFG in the framework of the cluster of excellence EXC 1056 “Center for Advancing Electronics Dresden (cfaed).

A. Wolf, P. Schulz, D. Öhmann, M. Dörpinghaus and G. Fettweis are with the Vodafone Chair Mobile Communications Systems, Technische Universität Dresden, Dresden, Germany, E-mails: {albrecht.wolf, philipp.schulz2, david.oehmann, meik.doerpinghaus, gerhard.fettweis}@tu-dresden.de.

of multiple so-called component carriers. CA and DC also support non-collocated deployments. As indicated before, existing realizations of MC are mainly used for enhancing data rates, i.e., different information is transmitted over each individual branch (multiplexing). However, multiple connections can also be utilized to enhance the reliability, i.e., the same information is transmitted over all branches in parallel (diversity).

Recently, research on URLLC is emerging considerably; nevertheless, there are only a few works focusing on a detailed analysis of MC and its impact on reliability. In [8], [9], it is concluded that packet duplication across multiple connections is a suitable technique to achieve high reliability. Pocić et al. evaluate intra-frequency MC in system simulations to illustrate how the signal-to-interference-noise ratio and the reliability is improved [10]. Furthermore, Tesema et al. demonstrate that mobility problems can be resolved by utilizing intra-frequency MC, see [11]. In another work by Nielsen and Popovski, multi-radio access-technology architectures are compared regarding their latency, which is significantly improved by MC techniques [12].

Motivated by the potential of MC to satisfy the URLLC requirements, we investigate a system and channel model that complies with MC architectures. The multiple diversity branches that correspond to an orthogonal multiple access channel (MAC) are realized by different carrier frequencies. Thus, the information can, in the best case, be delivered in a single time slot, which helps satisfying the URLLC requirements.

### B. Combining Algorithms

Combining algorithms merge the information received by multiple inputs (diversity branches) to a single unified output. The goal is to make use of the redundant information received from multiple inputs. There are various combining algorithms known in literature [13]–[15], of which many merge the received inputs at the symbol level, e.g.:

- 1) *Maximum Selection Combining*, where the “best” received input at the symbol level is selected, while all other received inputs are discarded.
- 2) *Maximum Ratio Combining*, where all received inputs are coherently combined at the symbol level.

In contrast to MSC and MRC which combine inputs already at the symbol level, the concept of

- 3) *Joint Decoding* is to combine the received inputs by exchanging information between the decoders of each branch, i.e., the received inputs are combined at the decoder level.

In addition to the different combining levels, JD differs fundamentally from MSC and MRC in that the encoders at the transmitter side produce different channel codewords, while MSC and MRC combine received inputs from the same channel codeword. The performance of MSC and MRC has been very well studied in various contexts [13]–[15], whereas to the best of our knowledge the performance of JD has not yet been quantified in the context of MC.

### C. Outage Analysis for Joint Decoding

The performance improvement of JD can be studied based on multiterminal source coding (also referred to as distributed source coding). Slepian and Wolf [16] were the first to characterize the problem of distributed encoding of multiple correlated sources. In their seminal paper, the rate region for the lossless distributed encoding of two correlated sources was derived.

Motivated by the capabilities of practical JD schemes (see, e.g., [17]–[19]) Matsumoto et al. established an analytical framework to evaluate their performance. In [20], [21] the JD outage performance was analyzed for a three-node decode-and-forward relaying system allowing intra-link errors (DF-IE). The analysis was based on multiterminal source coding and the source-channel separation theorem [22, Th. 3.7] yielding a multiterminal source-channel coding setup. In [23] and [24] the analysis was extended to a DF-IE system model with an arbitrary number of relays, with and without a direct link between source and destination, respectively.

### D. SNR Gain and Diversity-Multiplexing Tradeoff

In this work, we compare the performance of JD to MSC and MRC by two metrics, namely the SNR gain and the DMT, which we outline in the following.

A convenient way to analyze the JD performance improvement is to evaluate the required transmit power of JD, MSC, and MRC achieving a given target outage probability. Eventually, we are interested in the transmit power offset between JD and MSC/MRC, which we refer to as SNR gain. However, even though the SNR gain is an effective metric to quantify the performance improvement, it neglects certain aspects.

In most wireless communication systems, a demand for contradictory requirements exists: high transmission reliability (diversity gain) and high data rates (multiplexing gain). In general, improving transmission reliability usually results in a decreased data rate and vice versa. Therefore, it is crucial to balance these two contradictory requirements. Motivated by this, in the seminal work of Zheng and Tse [25], it has been proven that a multiple-input multiple-output (MIMO) system can also be used to increase the aforementioned gains simultaneously with a tradeoff. This tradeoff is referred to as DMT, where it is proven that at multiplexing gain  $r$  the diversity gain  $d$  will not exceed  $d(r)$ . The DMT states that by doubling the SNR we get both a decrease of outage probability scaled by  $2^{-d(r)}$  yielding an increase in reliability and  $r$  additional bits per channel use. The DMT has always been serving as the benchmark for comparing existing schemes to new schemes. Since the MC system

model can be considered as a MIMO wireless system with diagonal channel matrix, it is reasonable to compare JD, MSC and MRC based on the DMT as well. It is known that for the MC system model the maximum diversity gain and the maximum multiplexing gain are equal to the number of links, cf. [26]<sup>1</sup>.

To the best of our knowledge no existing publication addressed DMT of JD in the context of MC, where (a) one source is differently encoded based on a joint codebook and transmitted over an inter-frequency orthogonal MAC to achieve high reliability, and (b) multiple carrier frequencies are used to cope with low latency constraints.

### E. Contributions of this Work

Inspired by the JD outage probability analysis in [20], [21], this paper aims to develop a better understanding of the SNR gain and fundamental DMT of JD in block-fading orthogonal MACs in the context of MC. The contributions of this paper include the following:

- 1) We unify the outage probability derivations for JD, MRC and MSC by considering the MC architecture as a multiterminal source-channel coding setup, i.e., we perform a *rate analysis*. We establish a remarkably simple, yet accurate analytical description of the outage probabilities depending on the number of links  $N$ , spectral efficiency  $R_c$ , and received SNRs  $\Gamma_i$ , for  $i \in \{1, 2, \dots, N\}$ .
- 2) We prove that the SNR gains of JD  $G_{\text{JD}}$ , depend on the number of links  $N$  and the spectral efficiency  $R_c$ , and are given by

$$G_{\text{JD,MSC}} = f(R_c, N) > \sqrt[N]{N!}, \quad \text{and} \quad G_{\text{JD,MRC}} = \frac{1}{\sqrt[N]{N!}} f(R_c, N) > 1, \quad \text{with}$$

$$f(R_c, N) = \frac{2^{R_c} - 1}{\sqrt[N]{(-1)^N (1 - 2^{R_c} \cdot e_N(-R_c \ln(2)))}},$$

for MSC and MRC, respectively. Here,  $e_N(\cdot)$  is the exponential sum function. We show that JD becomes more advantageous with increasing spectral efficiency  $R_c$  as well as number of links  $N$ , i.e.,  $f(R_c, N)$  is an increasing function in  $R_c$  and  $N$ .

- 3) Moreover, we show that the JD DMT can achieve the maximum diversity gain as well as the maximum multiplexing gain for a block-fading orthogonal MAC of  $N$  links, i.e., the JD diversity gain is

$$d_{\text{JD}}(r) = N - r,$$

at a given multiplexing gain  $r \in [0, N]$ . By contrast, the MSC and MRC DMT can merely achieve the maximum diversity gain, i.e., the diversity gain is

$$d_i(r) = N \cdot (1 - r),$$

for  $i \in \{\text{MSC, MRC}\}$  at a given multiplexing gain  $r \in [0, 1]$ .

- 4) Furthermore, we illustrate the JD performance gain by comparison of the system throughput while achieving the same target outage probability for the different combining algorithms.

The performance metrics in 2), 3), and 4) provide a comprehensive evaluation of the gain of JD. The metrics in 2) and 4) describe the SNR offset between outage probabilities and system throughputs, and the metric in 3) describes the *pre-log* factor of the outage probability and system throughput at high SNR for all three combining algorithms.

- 5) Furthermore, we apply our outage analysis to real field channel measurements and thereby illustrate the potential of MC in actual cellular networks to achieve high reliability.

### F. Notation and Terminology

The upper- and lowercase letters are used to denote random variables (RVs) and their realizations, respectively, unless stated otherwise. The alphabet set of a RV  $X$  with realization  $x$  is denoted by  $\mathcal{X}$ , and its cardinality, respectively by  $|\mathcal{X}|$ . The probability mass function (pmf) and probability density function (pdf) of the discrete and continuous RV  $X$  is denoted by  $p_X(x)$  and  $f_X(x)$ , respectively. The pmf and pdf is simply denoted by  $p(x)$  and  $f(x)$ , respectively, whenever this notation is unambiguous. Also,  $\mathbf{X}^n$  and  $\mathbf{x}^n$  represent vectors containing a temporal sequence of  $X$  and  $x$  with length  $n$ , respectively. We use  $t$  to denote the time index and  $i$  to denote a source index. We define  $\mathbf{A}_{\mathcal{S}} = \{\mathbf{A}_i | i \in \mathcal{S}\}$  as an indexed series of random vectors, and  $A_{\mathcal{S}} = \{A_i | i \in \mathcal{S}\}$  as an indexed series of RVs. In general, a set  $\mathbf{A}$  contains elements  $a_{(\cdot)}$ , as in  $\mathbf{A} = \{a_1, a_2, \dots, a_{|\mathbf{A}|}\}$ . We define one particular set:  $\mathcal{N} = \{1, 2, \dots, N\}$ . We denote the Laplace transform of  $f(x)$  as  $\mathcal{L}_x[f(x)](p)$ , the probability of an event  $\mathcal{E}$  as  $\Pr[\mathcal{E}]$ , the convolution as  $*$ , the binary logarithm as  $\text{ld}(\cdot)$ , and the natural logarithm as  $\ln(\cdot)$ .

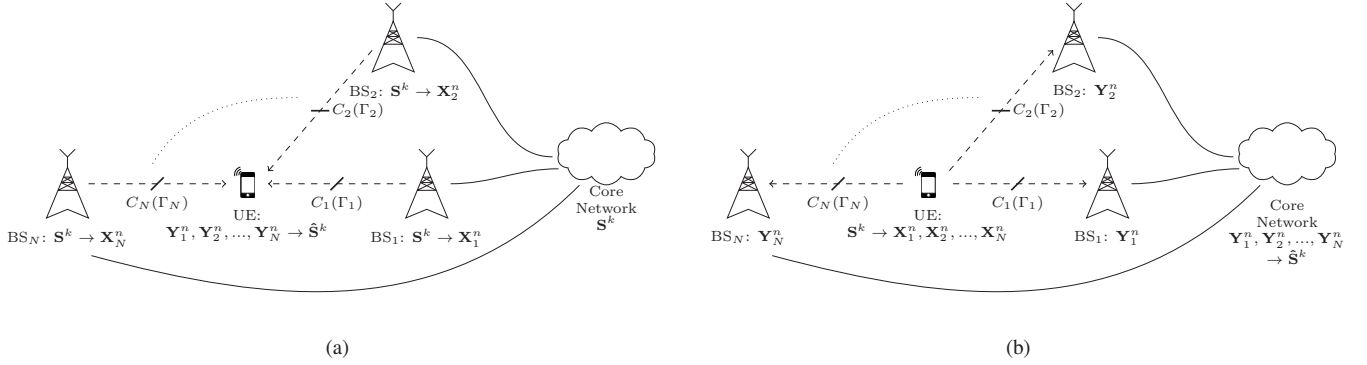


Fig. 1: System model with a single UE,  $N$  base stations, and a core network for (a) the downlink and (b) the uplink.

## II. SYSTEM MODEL

### A. Multi-Connectivity System Model

We consider a MC cellular network consisting of a core network and  $N$  base stations ( $\text{BS}_i, \forall i \in \mathcal{N}$ ) communicating to a single user equipment (UE). The core network coordinates the data transmissions to the UE. Connections between the core network and each BS are realized by backhaul links, and connections between each BS and UE by wireless links. By assumption all  $N$  wireless links are orthogonal, i.e., we consider an orthogonal MAC. The achievable transmission rate over the  $i$ th wireless link depends on its capacity  $C_i(\Gamma_i)$  and, thus, on its received SNR  $\Gamma_i$ . In the system model, we distinguish between down- and uplink as follows:

*a) Downlink:* The downlink system model, as illustrated in Fig. 1a, has one binary memoryless source, denoted as  $[S(k)]_{k=1}^{\infty}$ , with the  $k$ -sample sequence being represented in vector form as  $\mathbf{S}^k = [S(1), S(2), \dots, S(k)]$ . When appropriate, for simplicity, we shall drop the temporal index of the sequence, denoting the source merely as  $S$ . By assumption  $S$  takes values in a binary set  $\mathcal{B} = \{0, 1\}$  with uniform probabilities, i.e.,  $\Pr[S = 0] = \Pr[S = 1] = 0.5, \forall i \in \mathcal{N}$ . Therefore the entropy of the sequence is

$$1/k \cdot H(\mathbf{S}^k) = H(S) = 1. \quad (1)$$

The source sequence  $\mathbf{S}^k$  originating from the core network is encoded at  $N$  BSs. The  $i$ th transmit sequence at  $\text{BS}_i$ , denoted as  $\mathbf{X}_i^n$ , is sent to the UE over an orthogonal MAC. The decoder at the UE retrieves the source sequence  $\mathbf{S}^k$  from the received sequences  $\mathbf{Y}_i^n, \forall i \in \mathcal{N}$ .

*b) Uplink:* The uplink system model, as illustrated in Fig. 1b, is similar to the downlink, except that the source sequence is originated from the UE, and the received sequences  $\mathbf{Y}_i^n, \forall i \in \mathcal{N}$ , are decoded at the core network to retrieve the source sequence  $\mathbf{S}^k$ . Similar to the downlink, the  $i$ th transmit sequence  $\mathbf{X}_i^n$  is sent from the UE to the  $i$ th BS over an orthogonal MAC.

In this work, the down- and uplink system model can be considered as identical and all further results are applicable to both system models.

### B. Link Model

Instead of sending multiple sequences at different time slots to realize an orthogonal MAC, i.e., coding in time, we use multiple frequency channels to transmit the sequences. Thus, the sequences can, in the best case, be delivered in a single time slot, which helps satisfying the URLLC requirements. The frequency channels can be realized by using different channels within a single frequency band or, alternatively, by using channels of different frequency bands, c.f. inter-frequency MC in Section I. According to [27], the small-scale fading of two signals is approximately uncorrelated if their frequencies are at least separated by the coherence bandwidth, which is confirmed, for instance, by measurement results in [28]. In the following, we assume that the used frequency resources are at least separated by the coherence bandwidth. Thus, the channels are orthogonal and fade independently. Furthermore, to cope with the low latency constraint in URLLC, we consider relatively short encoded sequences. As a result, the length of an encoded sequence is less than or equal to the length of a fading block of a block Rayleigh fading. Moreover, the signals are transmitted from or to different BSs, which leads to individual average SNR values.

As argued, we can assume that the sequences  $\mathbf{X}_i^n, \forall i \in \mathcal{N}$ , are transmitted (in up- and downlink) over independent channels undergoing block Rayleigh fading and additive white Gaussian noise (AWGN) with mean power  $N_0$ . The pdf of the received SNR  $\Gamma_i$  is given by

$$f_{\Gamma_i}(\gamma_i) = \frac{1}{\Gamma_i} \exp\left(-\frac{\gamma_i}{\Gamma_i}\right), \quad \text{for } \gamma_i \geq 0, \quad (2)$$

<sup>1</sup>Note that Tse and Viswanath use a different scaling of the multiplexing gain, i.e., the multiplexing gain is normalized to the number of links.

with the average SNR  $\bar{\Gamma}_i$  being obtained as

$$\bar{\Gamma}_i = \frac{P_i}{N_0} \cdot d_i^{-\eta}, \quad (3)$$

where  $P_i$  is the transmit power per channel,  $d_i$  is the distance between BS<sub>*i*</sub> and the UE, and  $\eta$  is the path loss exponent. The channel state information is assumed to be known at the receiver.

The total transmit power  $P_T$  is equally allocated to all channels such that  $P_i = 1/N P_T, \forall i \in \mathcal{N}$ . Then, from (3) the average received SNR at the receiver can be written as

$$\bar{\Gamma}_i = \frac{1}{N} \frac{P_T}{N_0} \cdot d_i^{-\eta}. \quad (4)$$

We define the average system transmit SNR as  $P_T/N_0$ , i.e., normalizing all distances  $d_i$  to one. We shall use the total transmit power constraint for comparison of different configurations later on.

### III. PROBLEM STATEMENT AND APPROACH

The problem investigated in the work corresponds to a multiterminal channel coding problem, i.e., the received channel codewords  $\mathbf{Y}_1^n, \dots, \mathbf{Y}_N^n$  (cf. received sequences in Section II-A) must comprise sufficient information such that the source sequence  $\mathbf{S}^k$  can be perfectly reconstructed with a given outage probability  $\Pr[\mathbf{S}^k \neq \hat{\mathbf{S}}^k]$ . At each terminal, a channel code maps the source sequence  $\mathbf{S}^k$  to a channel codeword  $\mathbf{X}_i^n$  (cf. transmitted sequence in Section II-A) with the spectral efficiency  $R_{i,c}$ , measured in source samples per channel input symbol, associated with

- the modulation scheme  $R_{i,M} = \text{ld}(M)$ , measured in bits per channel input symbol with the cardinality  $M$  of the channel input symbol alphabet; and
- the channel code rate  $R_{i,\text{cod}}$ , measured in source samples per bit;

i.e.,  $R_{i,c} = R_{i,M} \cdot R_{i,\text{cod}}$ .

*Problem Statement:* Find the set of  $N$ -tuples  $R_{1,c}, \dots, R_{N,c}$  such that the received channel codewords  $\mathbf{Y}_1^n, \dots, \mathbf{Y}_N^n$  comprise sufficient information to perfectly reconstruct the source sequence  $\mathbf{S}^k$  with a given outage probability  $\Pr[\mathbf{S}^k \neq \hat{\mathbf{S}}^k]$ .

The set of  $N$ -tuples  $R_{1,c}, \dots, R_{N,c}$  that satisfy the constraint formulated in the *problem statement* very much depends on the applied combining algorithms. Prior studies considering MSC and MRC are based on the analysis of the gain attained by receiving the same channel codeword via multiple links, i.e., the channel codewords are identical  $\mathbf{X}_1^n = \dots = \mathbf{X}_N^n$  implying that the spectral efficiencies are identical  $R_{i,c} = R_c, \forall i \in \mathcal{N}$ . At the receiver side the received channel codewords  $\mathbf{Y}_1^n, \dots, \mathbf{Y}_N^n$  are combined at the symbol level. MSC and MRC are very well studied combining algorithms for which the outage probability is obtained as follows [13]–[15]:

*Maximum selection combining:* The channel with the maximum SNR is selected, such that the channel capacity for MSC is given by  $C_{\text{MSC}} = \phi(\Gamma_{\max} = \max(\Gamma_1, \dots, \Gamma_N))$ , where  $\phi(x) = \text{ld}(1+x)$  is the instantaneous AWGN channel capacity. The corresponding received sequence  $\mathbf{Y}_i^n, i = \arg \max(\Gamma_1, \dots, \Gamma_N)$  is decoded to retrieve the source sequence  $\mathbf{S}^k$ . The probability that the source sequence  $\mathbf{S}^k$  cannot be perfectly reproduced  $\Pr[\mathbf{S}^k \neq \hat{\mathbf{S}}^k]$  can be derived based on the probability that the MSC channel capacity depending on the maximal SNR is less than the spectral efficiency, i.e.,  $\Pr[\phi(\Gamma_{\max}) < R_c]$  is the MSC outage probability. We refer to this approach as *SNR analysis*.

*Maximum ratio combining:* All received symbols are coherently added at the receiver side, so that  $C_{\text{MRC}} = \phi(\Gamma_{\text{MRC}} = \sum_{i=1}^N \Gamma_i)$  is the MRC channel capacity. The coherently added received sequence is decoded to retrieve the source sequence  $\mathbf{S}^k$ . Similar to MSC, the probability that the source sequence  $\mathbf{S}^k$  cannot be perfectly reproduced  $\Pr[\mathbf{S}^k \neq \hat{\mathbf{S}}^k]$  can be derived based on a *SNR analysis*, i.e., the outage event occurs if the MRC channel capacity depending on the combined SNRs is less than the spectral efficiency, i.e.,  $\Pr[\phi(\Gamma_{\text{MRC}}) < R_c]$  is the MRC outage probability.

On the other hand, for *joint decoding*, the channel codewords transmitted over all links are different but based on a joint codebook. As a consequence, the spectral efficiencies of the individual links can differ and the set of  $N$ -tuples  $R_{1,c}, \dots, R_{N,c}$  that satisfy the constraint formulated in the *problem statement* is more flexible allowing a tradeoff between diversity and multiplexing. To find the set of  $N$ -tuples  $R_{1,c}, \dots, R_{N,c}$  we reformulate the multiterminal channel coding problem into a multiterminal source-channel coding problem, which we refer to as *rate analysis*. This approach was initially proposed by Matsumoto et al in [20], [21] for a DF-IE system model. The idea of the *rate analysis* is to decouple the source and channel coding, where the multiterminal source coding defines the admissible set of source information allocations to each channel codeword. In the following, we refer to the source information allocations as transmission rates  $R_i, \forall i \in \mathcal{N}$ , measured in bits per source sample. The admissible set of  $N$ -tuples  $R_1, \dots, R_N$  can be found based on multiterminal source coding. The allocated source information is then encoded by a point-to-point channel code at each terminal. We can reason the optimality of the source-channel code decoupling by Shannon's source-channel separation theorem. In the following we outline the *rate analysis* in detail.

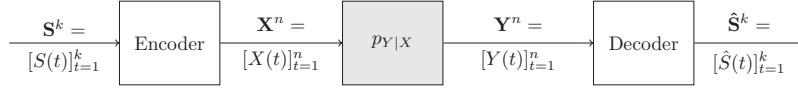


Fig. 2: Joint source-channel coding setup.

### A. Source-Channel Separation Theorem

Fig. 2 illustrates a joint source-channel (JSC) setup where the transmitter wishes to communicate  $k$  symbols of an uncompressed source  $S$  over a discrete memoryless channel  $p_{Y|X}$  in  $n$  transmissions so that the receivers can reconstruct the source symbols within a distortion constraint  $D$ . A prevalent way, in this case, is to perform source and channel encoding as well as channel and source decoding separately. For point-to-point communication with memoryless source and memoryless channel, Shannon proved that such strategy is asymptotically optimal, i.e., for  $k \rightarrow \infty$ , which is called Shannon's source-channel separation theorem.

**Theorem 1.** (Source-channel separation theorem [22, Th. 3.7]) *Given a discrete memoryless source  $S$ , an average distortion measure  $d(s, \hat{s})$  with rate-distortion function  $R(D)$  and a discrete memoryless channel with capacity  $C$ , the following statement holds.*

*If  $kR(D) \leq nC$ , then there exists a sequence of JSC codes such that*

$$\limsup_{k \rightarrow \infty} \mathbb{E} \left[ d(\mathbf{S}^k, \hat{\mathbf{S}}^k) \right] \leq D, \quad (5)$$

where  $k$  is the number of source samples and  $n$  is the number of channel input symbols.  $R(D)$  is expressed in bits per source sample and the capacity  $C$  is in bits per channel input symbol.

### B. Mapping: SNR to Rate

According to [22, Th. 3.7], [21] the maximum achievable value of the transmission rate  $R_i$  is related to the received SNR  $\Gamma_i$  based on the block Rayleigh fading assumption by

$$R_i = \frac{1}{k/n} C_i(\Gamma_i) = \frac{1}{R_{i,c}} \phi(\Gamma_i), \quad (6)$$

where the instantaneous capacity  $C_i(\Gamma_i)$  of an AWGN channel is given by  $\phi(\Gamma_i) = \text{ld}(1 + \Gamma_i)$ . If not otherwise stated, for simplicity, we shall assume  $R_{i,c} = R_c$ .

### C. Multiterminal Source Coding

Slepian and Wolf [16] considered a source coding problem where the decoder aims at perfectly reproducing two correlated sources which are independently compressed at two terminals. In their seminal paper, the rate region for this problem was derived. A simple proof of the Slepian-Wolf result with extension to an arbitrary number of sources was presented by Cover in [29].

**Theorem 2.** (Generalized Slepian-Wolf theorem [29]) *In order to achieve lossless compression of  $N$  correlated sources  $S_1, S_2, \dots, S_N$ , the source code rates  $R_i, \forall i \in \mathcal{N}$ , measured in bits per source sample, should satisfy the following conditions*

$$\sum_{i \in \mathcal{S}} R_i \geq H(\{S_i | i \in \mathcal{S}\} | \{S_j | j \in \mathcal{S}^c\}), \forall \mathcal{S} \subseteq \mathcal{N}, \quad (7)$$

where  $\mathcal{S}^c$  denotes the complement of  $\mathcal{S}$ .

The set of  $N$ -tuples  $R_1, \dots, R_N$  which satisfies all the constraints in (7) is referred to as the Slepian-Wolf rate region  $\mathcal{R}_{\text{SW}}$ . If all sources are identical, the Slepian-Wolf setup corresponds to the MC system model, i.e., the Slepian-Wolf rate region in (7) simplifies to

$$\sum_{i=1}^N R_i \geq H(S) = 1 \quad (8)$$

The set of  $N$ -tuples  $R_1, \dots, R_N$  which satisfies all the constraints in (8) is referred to as the JD rate region  $\mathcal{R}_{\text{JD}}$ .

### D. Rate Analysis

We apply the source-channel separation theorem to a multiterminal setup, as illustrated in Fig. 3 for two terminals ( $N = 2$ ). The multiterminal source-channel code is based on random coding and binning [22]. At each terminal the source sequence  $\mathbf{S}^k$  is compressed (source encoder) by transmission rate  $R_i$ , i.e., a bin  $b_i(\mathbf{s}^k) \in [1, \dots, 2^{kR_i}]$  for source outputs  $\mathbf{s}^k \in \mathcal{S}^k$  is randomly and independently assigned. The admissible rate region for the set of  $N$ -tuples  $R_1, \dots, R_N$  can be analyzed based on multiterminal source coding, cf. Section III-C. Then, a point-to-point channel code is applied with codebook  $\mathbf{x}_i^n(1), \dots, \mathbf{x}_i^n(b_i), \dots, \mathbf{x}_i^n(2^{kR_i})$ , such that  $C_{i,\text{JD}} = \phi(\Gamma_i)$  is the point-to-point JD channel capacity. The joint source decoder

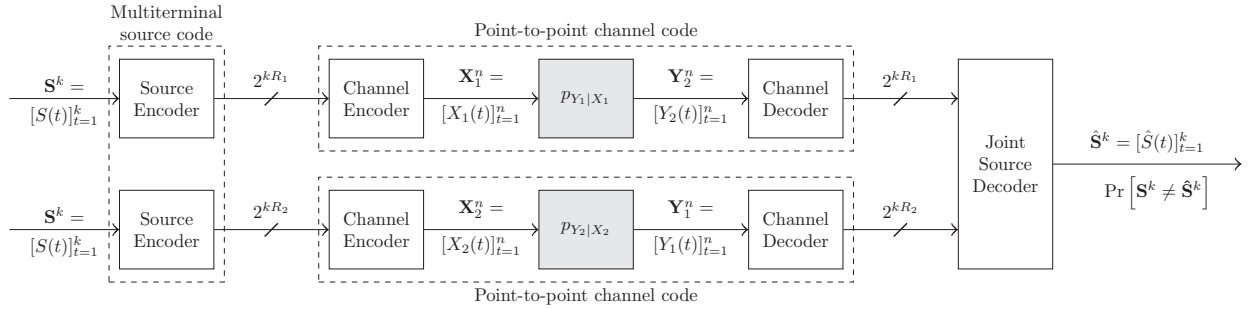


Fig. 3: Multiterminal source-channel coding setup.

reconstructs the source sequence  $\mathbf{s}^k$  based on the received channel codeword bins  $\mathbf{y}_1^n(b_1), \dots, \mathbf{y}_N^n(b_N)$ .

*Outage:* The event that the source sequence  $\mathbf{S}^k$  cannot be perfectly reproduced occurs if the set of achievable transmission rates does not satisfy the rate constraints of the admissible rate region in (8). The maximal achievable transmission rate of each link can be related to the SNR as in (6). Thus, the outage probability  $\Pr[\mathbf{S}^k \neq \hat{\mathbf{S}}^k]$  can be derived based on the admissible rate region (cf. Section III-C) and the SNR to rate mapping (cf. Section III-B), which we refer to as *rate analysis*.

Fig. 4 illustrates the JD *rate analysis* for  $N = 2$ . Let us assume that we have two received SNR realizations, i.e., the 2-tuple  $(\gamma_1, \gamma_2)$ . With (6) we can map the received SNR realizations into the transmission rate domain, i.e., the 2-tuple  $(\frac{1}{R_c} \cdot \phi(\gamma_1), \frac{1}{R_c} \cdot \phi(\gamma_2))$ . In Fig. 4 we marked two different 2-tuples at point *A* and point *B*. In addition, Fig. 4 illustrates the JD rate region  $\mathcal{R}_{\text{JD}}$  and its counterpart  $\mathcal{R}_{\text{JD}}^c$ . Both regions are separated from each other by the rate constraint in (8), i.e.,  $R_1 + R_2 = 1$ .

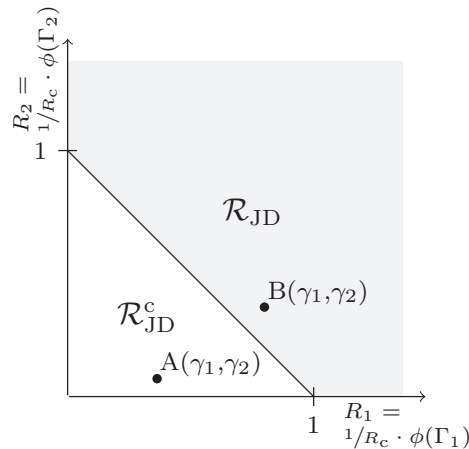


Fig. 4: JD rate region and SNR to rate mapping.

In summary, for MSC and MRC the outage probability can be derived based on a *max*- or *sum*-operation of the received SNRs (*SNR analysis*), whereas for JD an outage probability derivation must be established based on an admissible rate region analysis (*rate analysis*). However, the outage probability derivations can be unified, since MSC and MRC can be also analyzed based on a *rate analysis* as it shall soon become apparent. The outage probability derivation for MSC and MRC based on a *SNR analysis* is very well studied, e.g., [30], [31]. Hence, we can establish our *rate analysis* for MSC and MRC based on known results from the *SNR analysis* with some adjustments.

#### IV. OUTAGE PROBABILITIES

In this section, we derive the outage probability for JD, MSC, and MRC based on the *rate analysis* introduced in Section III. For JD we establish the exact outage probability in integral form. Unfortunately, the integral form cannot be solved in closed form. Thus, we give an approximation for the high SNR regime. For MSC and MRC we establish the exact outage probability in closed form based on known results from the *SNR analysis*. In addition, we give the approximated outage probability for MSC and MRC in closed form, which we require for the analysis at high SNR later on.

##### A. Joint Decoding

Considering JD, an outage event occurs whenever the transmission rate  $N$ -tuple  $R_1, \dots, R_N$  falls outside the JD rate region  $\mathcal{R}_{\text{JD}}$ . Using (6), the sum rate constraint in (8) which defines  $\mathcal{R}_{\text{JD}}$  can be mapped into a set of equivalent SNR constraints. Fig. 4 illustrates this approach for  $N = 2$ . The received SNR realizations, i.e., the 2-tuple  $(\gamma_1, \gamma_2)$  at point *A*, are transformed

into transmission rates, i.e., the 2-tuple  $(1/R_c \cdot \phi(\gamma_1), 1/R_c \cdot \phi(\gamma_2))$ . Since the transmission rate 2-tuple at point  $A$  is outside the JD rate region  $\mathcal{R}_{\text{JD}}$ , an outage event occurs, i.e., the joint decoder cannot perfectly reproduce the source sequence  $\mathbf{S}^k$ . The transmission rate 2-tuple at point  $B$  is inside the JD rate region  $\mathcal{R}_{\text{JD}}$ , i.e., the joint decoder can perfectly reproduce the source sequence  $\mathbf{S}^k$ . Thus, the outage probability for JD can be calculated as follows

$$P_{\text{JD},N}^{\text{out}} = \Pr[0 \leq R_1 + R_2 + \dots + R_N < 1] \quad (9a)$$

$$= \Pr[0 \leq \phi(\Gamma_1) + \phi(\Gamma_2) + \dots + \phi(\Gamma_N) < R_c] \quad (9b)$$

$$= \Pr[0 \leq \phi(\Gamma_1) < R_c, 0 \leq \phi(\Gamma_2) < R_c - \phi(\Gamma_1), \dots, \\ 0 \leq \phi(\Gamma_N) < R_c - \phi(\Gamma_1) - \phi(\Gamma_2) - \dots - \phi(\Gamma_{N-1})] \quad (9c)$$

$$= \Pr\left[0 \leq \Gamma_1 < 2^{R_c} - 1, 0 \leq \Gamma_2 < 2^{R_c - \phi(\Gamma_1)} - 1, \dots, \\ 0 \leq \Gamma_N < 2^{R_c - \phi(\Gamma_1) - \phi(\Gamma_2) - \dots - \phi(\Gamma_{N-1})} - 1\right] \quad (9d)$$

$$= \int_{\gamma_1=0}^{2^{R_c}-1} \int_{\gamma_2=0}^{2^{R_c-\phi(\gamma_1)}-1} \dots \int_{\gamma_N=0}^{2^{R_c-\phi(\gamma_1)-\phi(\gamma_2)-\dots-\phi(\gamma_{N-1})}-1} f(\gamma_1)f(\gamma_2)\dots f(\gamma_N)d\gamma_N\dots d\gamma_2d\gamma_1. \quad (9e)$$

The steps are justified as follows: (9a) is the constraint on the sum rate in (8); in (9b) the rate constraint is mapped into the SNR constraint with use of (6); in (9c) the sum constraint is separated into individual constraints; in (9d) the bounds are transformed with  $\phi^{-1}(y) = 2^y - 1$ ; in (9e) the probability of outage is established in integral form with the assumption that the received SNRs  $\gamma_i, \forall i \in \mathcal{N}$ , are independent. The pdf  $f(\gamma_i)$  is given in (2). Although the outage expression in (9e) cannot be solved in closed form, a simple asymptotic solution can be derived at high SNR as

$$P_{\text{JD},N}^{\text{out}} \approx \int_{\gamma_1=0}^{2^{R_c}-1} \int_{\gamma_2=0}^{2^{R_c-\phi(\gamma_1)}-1} \dots \int_{\gamma_N=0}^{2^{R_c-\phi(\gamma_1)-\phi(\gamma_2)-\dots-\phi(\gamma_{N-1})}-1} \frac{1}{\bar{\Gamma}_1\bar{\Gamma}_2\dots\bar{\Gamma}_N} d\gamma_N\dots d\gamma_2d\gamma_1 \quad (10a)$$

$$= \frac{A_N(R_c)}{\bar{\Gamma}_1\bar{\Gamma}_2\dots\bar{\Gamma}_N} \quad \text{where} \quad (10b)$$

$$A_N(R_c) = (-1)^N (1 - 2^{R_c} \cdot e_N(-R_c \ln(2))). \quad (10c)$$

Here,  $e_N(x) = \sum_{n=0}^{N-1} \frac{x^n}{n!}$  is the exponential sum function. For more details, we refer to the derivations in Appendix A. We will discuss the outage probability  $P_{\text{JD},N}^{\text{out}}$  based on numerical examples in Section VIII.

### B. Maximum Selection Combining

For MSC [30], at each time instance only the channel with the maximum transmission rate  $R_{\text{max}} = \max(R_1, R_2, \dots, R_N)$  is selected. If  $R_{\text{max}}$  does not satisfy the rate constraint for lossless compression, see, e.g., [32, Th. 10.3.1]

$$R_{\text{max}} \geq H(S) = 1, \quad (11)$$

an outage occurs. The outage probability for MSC can be derived as follows

$$P_{\text{MSC},N}^{\text{out}} = \Pr[0 \leq R_{\text{max}} < 1] \quad (12a)$$

$$= \Pr[0 \leq \phi(\Gamma_{\text{max}}) < R_c] \quad (12b)$$

$$= \Pr[0 \leq \phi(\Gamma_1) < R_c, 0 \leq \phi(\Gamma_2) < R_c, \dots, 0 \leq \phi(\Gamma_N) < R_c] \quad (12c)$$

$$= \Pr[0 \leq \Gamma_1 < 2^{R_c} - 1, 0 \leq \Gamma_2 < 2^{R_c} - 1, \dots, 0 \leq \Gamma_N < 2^{R_c} - 1] \quad (12d)$$

$$= \prod_{i=1}^N \int_{\gamma_i=0}^{2^{R_c}-1} f(\gamma_i)d\gamma_i \quad (12e)$$

$$= \prod_{i=1}^N \left(1 - \exp\left(-\frac{A_1(R_c)}{\bar{\Gamma}_i}\right)\right) \quad (12f)$$

with  $A_1(R_c) = 2^{R_c} - 1$ . The steps are justified as follows: (12a) is the constraint on the rate in (11); (12b) - (12d) follow the same arguments as in (9b), (9d), and (9e), respectively; in (12e) the multiple integral can be rewritten as the product of single integrals, since the integral domain in (12d) is normal and the SNRs are independent; (12f) is the closed-form solution of the integral in (12e). An asymptotic solution at high SNR can be derived by the MacLaurin series for the exponential function  $\exp(-x_i) \approx 1 - x_i$  for  $x_i \rightarrow 0$ , giving

$$P_{\text{MSC},N}^{\text{out}} \approx \left(\frac{A_1(R_c)}{\bar{\Gamma}}\right)^N, \quad \text{for } \bar{\Gamma}_1 = \dots = \bar{\Gamma}_N = \bar{\Gamma}. \quad (13)$$

### C. Maximum Ratio Combining

For MRC [30] all received symbols are coherently added. The sum of all symbols is then decoded. We can apply the point-to-point communication system assumption in Section III-A if we define an auxiliary RV, namely the total received SNR  $\Gamma_{\text{MRC}}$  as

$$\Gamma_{\text{MRC}} = \sum_{i=1}^N \Gamma_i. \quad (14)$$

The pdf of the received SNR  $\Gamma_{\text{MRC}}$  is given by

$$f_{\Gamma_{\text{MRC}}}(\gamma_{\text{MRC}}) = f_{\Gamma_1}(\gamma_1) * f_{\Gamma_2}(\gamma_2) * \dots * f_{\Gamma_N}(\gamma_N) \quad (15a)$$

$$= \mathcal{L}_p^{-1} [\mathcal{L}_{\gamma_1} [f_{\Gamma_1}(\gamma_1)](p) \cdot \mathcal{L}_{\gamma_2} [f_{\Gamma_2}(\gamma_2)](p) \cdot \dots \cdot \mathcal{L}_{\gamma_N} [f_{\Gamma_N}(\gamma_N)](p)](\gamma_{\text{MRC}}) \quad (15b)$$

$$= \frac{\gamma_{\text{MRC}}^{(N-1)}}{(N-1)! \cdot \bar{\Gamma}^N} \exp\left(-\frac{\gamma_{\text{MRC}}}{\bar{\Gamma}}\right). \quad (15c)$$

The steps are justified as follows: For (15a) the pdf of a sum of RVs is the convolution of their pdfs; for (15b) a convolution of functions is a multiplication of their Laplace transforms where  $\mathcal{L}_{\gamma_i} [f_{\Gamma_i}(\gamma_i)](p) = 1/(\bar{\Gamma}_i p + 1)$ . The result in (15c) holds for  $\bar{\Gamma}_1 = \dots = \bar{\Gamma}_N = \bar{\Gamma}$  which we assume for simplicity. With the total received SNR  $\Gamma_{\text{MRC}}$  we can assume a point-to-point communication system and thus the outage probability can be calculated as follows

$$P_{\text{MRC},N}^{\text{out}} = \Pr[0 \leq R_{\text{MRC}} < 1] \quad (16a)$$

$$= \Pr[0 \leq \phi(\Gamma_{\text{MRC}}) < R_c] \quad (16b)$$

$$= \Pr[0 \leq \Gamma_{\text{MRC}} < 2^{R_c} - 1] \quad (16c)$$

$$= \int_{\gamma_{\text{MRC}}=0}^{2^{R_c}-1} f(\gamma_{\text{MRC}}) d\gamma_{\text{MRC}} \quad (16d)$$

$$= 1 - \exp\left(-\frac{A_1(R_c)}{\bar{\Gamma}}\right) \left(\sum_{i=1}^N \frac{(A_1(R_c)/\bar{\Gamma})^{(i-1)}}{(i-1)!}\right) \quad (16e)$$

The steps can be justified similar to (12a) - (12e). The closed form of the integral in (16d) is given in [30, (2.33)]. An asymptotic solution can be derived at high SNR [31, (16)] as

$$P_{\text{MRC},N}^{\text{out}} \approx \frac{1}{N!} \left(\frac{A_1(R_c)}{\bar{\Gamma}}\right)^N. \quad (17)$$

### V. SNR GAIN

To quantify the performance gain of JD over MSC and MRC in terms of the outage probability, we evaluate the required average system transmit SNR  $P_T/N_0$ , cf. (4), to achieve a target outage probability  $P_*^{\text{out}}$  in the high SNR domain. Thus, we substitute (4) into (10b), (13) and (17) for JD, MSC and MRC, respectively, yielding

$$\frac{P_T}{N_0} = \sigma_i(P_*^{\text{out}}), \quad (18)$$

where  $\sigma_i(P_*^{\text{out}})$  is the required average system transmit SNR depending on  $P_*^{\text{out}}$  and the combining algorithm, where  $i \in \{\text{JD}, \text{MSC}, \text{MRC}\}$ . In order to examine the SNR gain provided by JD versus MRC and MRC, we consider the reduction of the required average system transmit SNR while achieving the same target outage probability. We define the SNR gain of JD as

$$G_{\text{JD},i} = \frac{\sigma_i(P_*^{\text{out}})}{\sigma_{\text{JD}}(P_*^{\text{out}})}, \quad \text{for } i \in \{\text{MSC}, \text{MRC}\}. \quad (19)$$

**Proposition 3.** *The SNR gains of joint decoding over maximum selection combining and maximum ratio combining in the high SNR range for  $R_c > 0$ ,  $N \in \mathbb{N} \setminus \{1\}$  are given by*

$$G_{\text{JD},\text{MSC}} = \frac{A_1(R_c)}{\sqrt[N]{A_N(R_c)}} > \sqrt[N]{N!}, \quad \text{and} \quad (20)$$

$$G_{\text{JD},\text{MRC}} = \frac{1}{\sqrt[N]{N!}} \cdot \frac{A_1(R_c)}{\sqrt[N]{A_N(R_c)}} > 1, \quad \text{respectively.} \quad (21)$$

*Proof.* We substitute  $\bar{\Gamma} = \frac{1}{N} \frac{P_T}{N_0} = \frac{1}{N} \sigma_i(P_*^{\text{out}})$  into (10b), (13), and (17). We then rearrange (10b), (13), and (17) and substitute the results into (19). Some algebraic manipulations yield (20) and (21). It is proven in Lemma 6 (see Appendix B) that  $A_1(R_c)/(\sqrt[N]{N!} \sqrt[N]{A_N(R_c)}) > 1$ , which implies that  $A_1(R_c)/\sqrt[N]{A_N(R_c)} > \sqrt[N]{N!}$ . This completes the proof.  $\square$

We will discuss the SNR gains of JD based on numerical examples in Section VIII. Furthermore, we will show in Section VIII that both SNR gains are increasing functions in  $R_c$  and  $N$ .

## VI. DIVERSITY-MULTIPLEXING TRADEOFF

In the context of MIMO systems [25], it is proven that for a multiplexing gain<sup>2</sup>

$$r = \lim_{\bar{\Gamma} \rightarrow \infty} \frac{R_c(\bar{\Gamma})}{\text{ld}(N\bar{\Gamma})}, \quad (22)$$

the diversity gain  $d$  will not exceed

$$d(r) = - \lim_{\bar{\Gamma} \rightarrow \infty} \frac{\text{ld} P_{\cdot, N}^{\text{out}}(r, \bar{\Gamma})}{\text{ld}(N\bar{\Gamma})}. \quad (23)$$

Since the MC system model can be considered as an  $N \times N$  MIMO system of  $N$  transmit and  $N$  receive antennas with a diagonal channel matrix, it is reasonable to compare JD, MSC and MRC based on the DMT as well. An optimal combining algorithm can achieve a maximum diversity gain and a maximum multiplexing gain of  $N$ , cf. [26]<sup>3</sup>.

**Theorem 4.** *For joint decoding and infinite SNR, the diversity gain is a function of the multiplexing gain given by*

$$d_{JD}(r) = N - r, \quad r \in [0, N]. \quad (24)$$

*The diversity-multiplexing tradeoff of joint decoding is optimal for an orthogonal multiple access channel with  $N$  wireless links. The diversity-multiplexing tradeoff for maximum selection combining and maximum ratio combining is given by*

$$d_i(r) = N \cdot (1 - r), \quad r \in [0, 1], \quad (25)$$

for  $i \in \{MSC, MRC\}$ , respectively.

*Proof.* See Appendix C. □

Fig. 5 illustrates the DMT for JD, MSC and MRC. JD can achieve a maximum multiplexing gain of  $N$ , whereas MSC and MRC merely can achieve a maximum multiplexing gain of 1. As an orthogonal MAC is assumed, the DMT of JD is optimal, i.e., JD achieves the maximum diversity gain as well as the maximum multiplexing gain.

*Remark:* In literature, the DMT of MRC and MSC is well studied for an orthogonal MAC [26]. In the context of MIMO

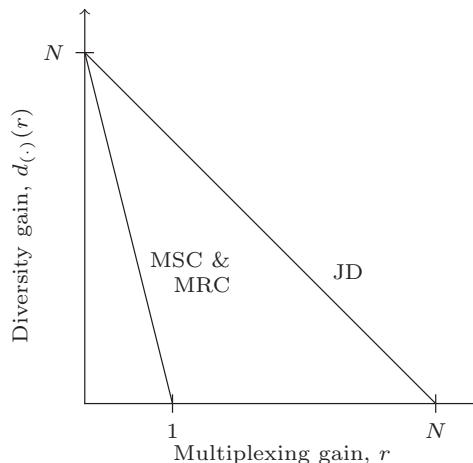


Fig. 5: DMT for JD, MSC, and MRC.

systems the diagonal channel matrix can be achieved by a repetition scheme<sup>4</sup>. We confirm that our results based on the *rate analysis* align with the results based on the *SNR analysis*.

The maximum multiplexing gain of JD can be reasoned with the “*sum over log*” operation for the received SNRs as shown in the following. Let us consider the SNR constraints in (9b) that define the JD outage for  $N = 2$ . We can reformulate (9b) to  $\phi(\Gamma_1) + \phi(\Gamma_2) \leq R_c$ , which is equal to  $\Gamma_1 \cdot \Gamma_2 + \Gamma_1 + \Gamma_2 \leq 2^{R_c} - 1$ . In contrast, for MRC the received SNRs are combined by a “*log over sum*” operation, i.e., the SNR constraint in (16b) that defines the MRC outage is  $\phi(\Gamma_1 + \Gamma_2) \leq R_c$ , which is equal to  $\Gamma_1 + \Gamma_2 \leq 2^{R_c} - 1$ . As one can easily see, the received SNRs are linearly added by MRC, i.e., the highest SNR order is 1 and so is its maximum multiplexing gain, whereas the received SNRs are multiplied by JD, i.e., the highest SNR order is  $N = 2$  and so is its maximum multiplexing gain. The same is true for an arbitrary number of links  $N$ .

<sup>2</sup> $N\bar{\Gamma}$  is the average system transmit SNR and  $\bar{\Gamma}$  the average transmit SNR per link.

<sup>3</sup>Note that Tse and Viswanath use a different scaling of the multiplexing gain, i.e., the multiplexing gain is normalized to  $N$ .

<sup>4</sup>The same channel codewords are transmitted over each channel in an orthogonal time domain.

## VII. SYSTEM THROUGHPUT

Although the DMT analysis is an effective measure to capture the system throughput *pre-log* factor at high SNR, we would like to evaluate the absolute value of the system throughput itself, i.e., how much information is received at the destination on average per transmission depending on the SNR. To capture this, following the standard approach in literature [13], we define the system throughput  $T$  as the product of the bandwidth  $B$ , spectral efficiency  $R_c$ , and the target non-outage probability  $(1 - P_*^{\text{out}})$  as

$$T_{i,N}(B, R_c, \bar{\Gamma}_N) = B \cdot R_c(i, N, \bar{\Gamma}_N) \cdot (1 - P_*^{\text{out}}) \text{ in bit/s,} \quad (26)$$

for  $i \in \{\text{JD, MSC, MRC}\}$ . To evaluate (26) we require the achieved spectral efficiency  $R_c(i, N, \bar{\Gamma}_N)$  for the different combining algorithms ( $i \in \{\text{JD, MSC, MRC}\}$ ) for a given number of links  $N$  and average received SNRs  $\bar{\Gamma}_N$ .  $R_c(i, N, \bar{\Gamma}_N)$  can be calculated by the outage probability framework established before, i.e., by reformulating (10b), (12f), and (16e). We illustrate the achieved system throughput for different numbers of links, average system transmit SNR, and target outage probabilities for JD, MSC, and MRC by numerical examples in Section VIII.

## VIII. NUMERICAL RESULTS

In this section, we illustrate and discuss the exact and asymptotic outage probabilities, the SNR gain, and the system throughput of JD by numerical examples. For the purpose of illustration, we assume a path loss exponent of  $\eta = 3.5$ , and a bandwidth of  $B = 20$  MHz. To ensure a fair comparison, we make use of the total transmit power constraint in (4), i.e., the transmit power is equally allocated to all links, such that  $P_i = P_T/N$ .

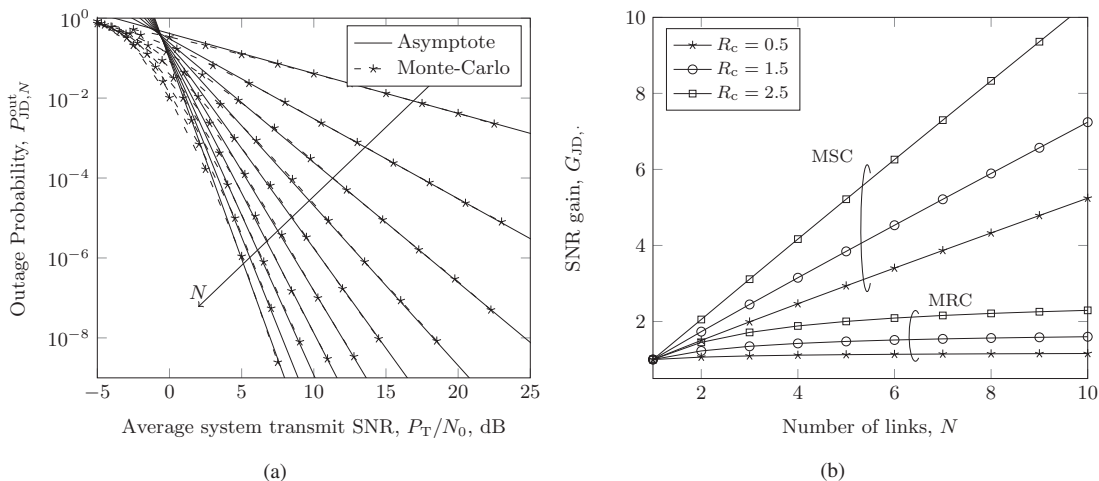


Fig. 6: (a) Exact and asymptotic JD outage probability with  $N \in \{1, 2, \dots, 10\}$  and  $R_c = 0.5$ , and (b) gain of required average system transmit SNR for target outage probability with respect to MSC and MRC.

Fig. 6a depicts the exact and asymptotic outage probability  $P_{\text{JD},N}^{\text{out}}$  defined previously in (9e) and (10b), respectively, versus the average system transmit SNR  $P_T/N_0$ . We show results for different numbers of links ( $N \in \{1, 2, \dots, 10\}$ ) and a constant spectral efficiency of  $R_c = 0.5$ . The following can be observed: (i) our asymptotic expression in (10b) is tight at medium to high SNR; and (ii) with every additional link the diversity gain  $d_{\text{JD}}(r)$  increases by one with constant spectral efficiency, i.e. the multiplexing gain is  $r = 0$ .

Fig. 6b depicts the SNR gain of JD  $G_{\text{JD},i}$  given in (20) and (21) in comparison to MSC and MRC, respectively, versus the number of links. The following can be observed: (i) the SNR gain of JD in (20) and (21) is greater than one for  $R_c \in \{0.5, 1.5, 2.5\}$  and  $N \in \{2, 3, \dots, 10\}$  as proven in Proposition 3; (ii) the SNR gain of JD increases with  $N$  and  $R_c$ ; and (iii) the SNR gain of JD with respect to MRC differs from the SNR gain of JD with respect to MSC by  $1/\sqrt[3]{N!}$ .

Fig. 7 depicts the system throughput  $T_{i,N}(B, R_c, \bar{\Gamma}_N)$  in (26) versus the average system transmit SNR  $P_T/N_0$ . In Fig. 7a we show the system throughput for different numbers of links  $N \in \{3, 8\}$  and a target outage probability of  $P_*^{\text{out}} = 10^{-5}$ . In Fig. 7b we show the system throughput for different target outage probabilities  $P_*^{\text{out}} \in \{10^{-5}, 10^{-10}\}$  and  $N = 8$  links. The following can be observed: (i) for increasing SNR, the JD system throughput increases asymptotically with  $N$  bits/s whereas the MSC and MRC system throughput increases asymptotically with 1 bits/s, which corresponds to the maximum multiplexing gains; (ii) the system throughputs of MSC and MRC have a constant offset; and (iii) a decrease in target outage probability manifests itself as a parallel shift of the respective system throughput curves, i.e. a uniform decrease independent of the transmit SNR.

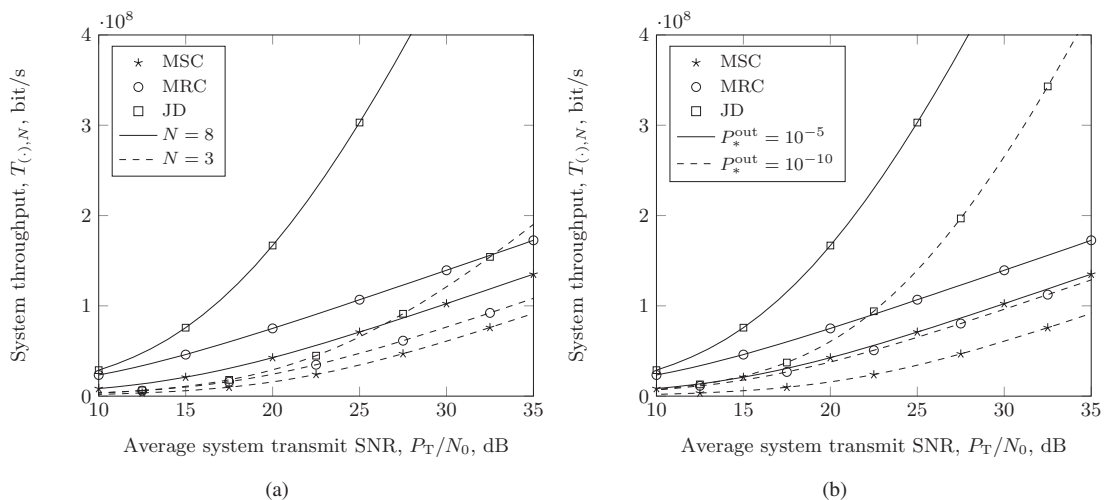


Fig. 7: System throughput for JD, MSC, and MRC; (a) for a target outage probability of  $P_*^{\text{out}} = 10^{-5}$  and different number of links  $N$ ; and (b) for number of links of  $N = 8$  and different target outage probabilities  $P_*^{\text{out}}$ .

## IX. CELLULAR FIELD TRIAL FOR UPLINK

In [33] measurements were carried out in a field trial testbed in Dresden (Germany) downtown. We make use of this measurement data to show the potential of MC in a real cellular network. In the field trial the uplink was considered. In this section, we shortly introduce the field trial setup and then present the empirical outage probability cumulative distribution function (CDF) for the measurement data. Our results elaborate on the following points: (i) the performance improvement if multiple links are included in the transmission and (ii) the performance gain of JD in comparison to MSC and MRC.

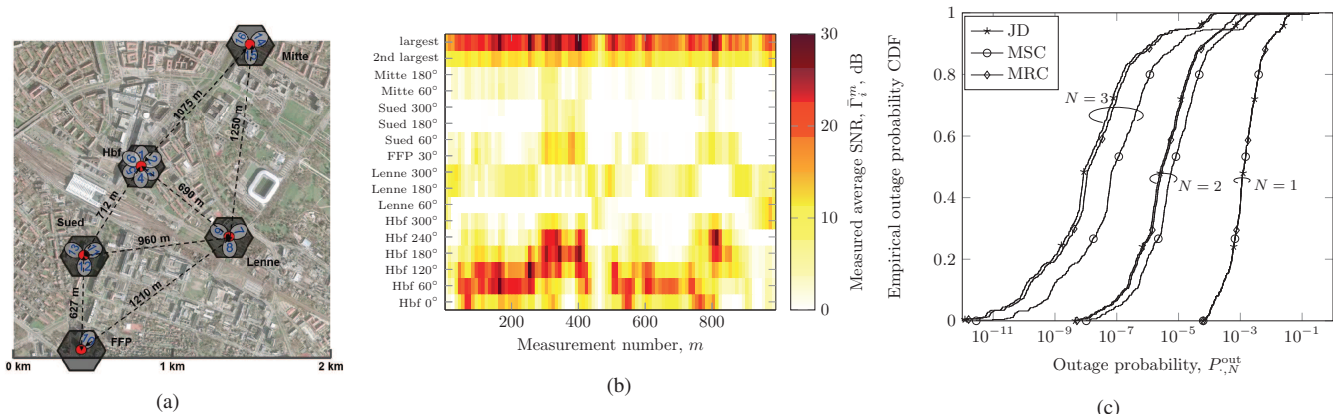


Fig. 8: (a) Testbed deployment, (b) measured average SNR  $\bar{\Gamma}_i^m$  achieved at all BSs of the testbed during the complete field trial [33], and (c) empirical outage probability CDF ( $N \in \{1, 2, 3\}$ ) for JD, MSC and MRC.

### A. Field Trial Setup

The field trial testbed, deployed in Dresden downtown, is depicted in Fig. 8a. In total, 16 BSs located on five sites with up to six-fold sectorization are used for the measurements. During the field trial, two UEs were moved on a measurement bus in 5 m distance while transmitting on the same time and frequency resources employing one dipole antenna each. The superimposed signal is jointly received by all BSs which took snapshots of 80 ms (corresponding to 80 transmit time intervals) every 10 s. In total about 1900 such measurements were taken in order to observe a large number of different transmission scenarios. In Fig. 8b the measured average SNR  $\bar{\Gamma}_i^m$  values for around 1000 measurements observed at all BSs and locations are shown, where  $m$  denotes the measurement number and  $i$  the BS index,  $i \in \{\text{Hbf } 0^\circ, \text{Hbf } 60^\circ, \dots\}$ . The two largest average SNRs measured at any BS for each measurement are depicted in the upper part of the figure. An interesting result is that multiple relatively high average SNR values of two different BSs are observed at each location of the UEs. Since combining algorithms are particularly beneficial in scenarios with multiple relatively high average SNR values, the result indicates that cooperation among BSs can improve reliable data transmission as will be presented in the next section. For more details on this field trial setup, please refer to [33].

### B. Empirical Outage Probability CDF

With the measured average SNR  $\bar{\Gamma}_i^m$  in Fig. 8b we can generate an empirical outage probability CDF. For each measurement we consider the  $N$  strongest links, i.e., the largest measured average SNRs  $\bar{\Gamma}_i^m$ . The outage probability can be assessed with (10b), (12f) and (16d) for JD, MSC and MRC, respectively, for each measurement. For MRC we have to calculate the pdf of the received SNR  $\Gamma_{\text{MRC}}$  in (15b), since the results in (15c) holds iff the average SNRs  $\bar{\Gamma}_i$  are equal. The pdf in (15b) for the received SNR  $\Gamma_{\text{MRC}}$  with  $N = 2$  and  $N = 3$  is

$$f_{\Gamma_{\text{MRC}}}(\gamma_{\text{MRC}}) = \frac{\exp(-\gamma_{\text{MRC}}/\bar{\Gamma}_1)}{\bar{\Gamma}_1 - \bar{\Gamma}_2} + \frac{\exp(-\gamma_{\text{MRC}}/\bar{\Gamma}_2)}{\bar{\Gamma}_2 - \bar{\Gamma}_1} \quad \text{and} \quad (27)$$

$$f_{\Gamma_{\text{MRC}}}(\gamma_{\text{MRC}}) = \frac{\bar{\Gamma}_1 \exp(-\gamma_{\text{MRC}}/\bar{\Gamma}_1)}{(\bar{\Gamma}_1 - \bar{\Gamma}_2)(\bar{\Gamma}_1 - \bar{\Gamma}_3)} + \frac{\bar{\Gamma}_2 \exp(-\gamma_{\text{MRC}}/\bar{\Gamma}_2)}{(\bar{\Gamma}_2 - \bar{\Gamma}_1)(\bar{\Gamma}_2 - \bar{\Gamma}_3)} + \frac{\bar{\Gamma}_3 \exp(-\gamma_{\text{MRC}}/\bar{\Gamma}_3)}{(\bar{\Gamma}_3 - \bar{\Gamma}_1)(\bar{\Gamma}_3 - \bar{\Gamma}_2)}, \quad (28)$$

respectively. By substituting (27) and (28) into (16d) we can numerically calculate the outage probability for MRC. Moreover, we evaluate the empirical outage probability CDF for JD, MSC and MRC with all measured average SNRs using (10b), (12f), and (16d), respectively.

Fig. 8c depicts the empirical outage probability CDF for different number of links with JD, MSC and MRC. The following can be observed: (i) with an increasing number of links the outage probability decreases; (ii) JD outperforms MSC and MRC; and (iii) with additional links the performance gain of JD increases.

### C. Discussion

Based on the field trial setup, we can conclude that MC can achieve a substantial performance improvement in real cellular networks. The measurement data at hand documents that multiple relatively high average SNR values frequently occur for which combining algorithms are particularly beneficial. From the uplink measurement data we can also draw conclusions for the downlink. As argued in Section II-B the statistical properties of the link model are identical for the up- and downlink. Thus, if the measurement data at hand documents that multiple relatively high average SNR values frequently occur in the uplink, it is reasonable to assume that multiple relatively high average SNR values frequently occur in the downlink as well. Based on this insight, MC can also achieve low outage probabilities in real cellular networks considering the downlink. Depending on the user requirements, our DMT analysis allows the network to adjust the system configurations.

## X. CONCLUSION

In this work, we have investigated the three combining algorithms joint decoding, maximum selection combining, and maximum ratio combining in the context of multi-connectivity architectures, i.e., the same information is encoded at multiple terminals and transmitted over an orthogonal MAC. To evaluate their performance, we have analytically described the outage probability depending on the number of links, the spectral efficiency, and the received signal-to-noise ratio based on a multiterminal source-channel coding setup. We have compared the performance of the three combining algorithms by the following metrics:

- 1) *SNR gain*: We have found, assuming equal noise power, that joint decoding requires less transmit power than maximum selection combining and maximum ratio combining to achieve a given target outage probability. Our analysis has revealed that the gain of joint decoding grows with an increasing number of links as well as increasing spectral efficiency.
- 2) *Diversity-multiplexing tradeoff*: It is known that the maximum diversity gain and the maximum multiplexing gain are equal to the number of links when considering an orthogonal multiple access channel. We have proven that joint decoding can achieve these maximum gains. By contrast, maximum selection combining and maximum ratio combining can merely achieve the maximum diversity gain but not the maximum multiplexing gain.
- 3) *System throughput*: We have evaluated the system throughput for all three combining algorithms depending on the number of links and different target outage probabilities. Thereby, we have shown the impact of the multiplexing gain but also the SNR offset between system throughputs for the different combining algorithms.

The three metrics provide a comprehensive evaluation of the gain of joint decoding over maximum selection combining and maximum ratio combining. The SNR offset between outage probabilities and system throughputs can be evaluated by metric in 1) and 3), respectively. In addition, metric 2) compactly describes the *pre-log* factor of the outage probability and system throughput at high SNR for all three combining algorithms.

In addition, we have applied the analytical framework for the outage probabilities of the aforementioned combining algorithms to real cellular networks. Based on the measurement data recorded in a field trial we have evaluated the achievable performance improvement by the use of multi-connectivity. The measurement data documents that multiple relatively high average SNR values frequently occur, in which case in which multi-connectivity is particularly beneficial.

APPENDIX A  
ASYMPTOTIC JOINT DECODING OUTAGE PROBABILITY

The asymptotic outage probability can be obtained as

$$P_{\text{JD},N}^{\text{out}} = \int_{\gamma_1=0}^{2^{R_c}-1} \int_{\gamma_2=0}^{2^{R_c-\phi(\gamma_1)}-1} \dots \int_{\gamma_N=0}^{2^{R_c-\phi(\gamma_1)-\phi(\gamma_2)-\dots-\phi(\gamma_{N-1})}-1} \frac{1}{\Gamma_1} \exp\left(-\frac{\gamma_1}{\Gamma_1}\right) \frac{1}{\Gamma_2} \exp\left(-\frac{\gamma_2}{\Gamma_2}\right) \dots \frac{1}{\Gamma_N} \exp\left(-\frac{\gamma_N}{\Gamma_N}\right) d\gamma_N \dots d\gamma_2 d\gamma_1 \quad (29a)$$

$$\approx \int_{\gamma_1=0}^{2^{R_c}-1} \int_{\gamma_2=0}^{2^{R_c-\phi(\gamma_1)}-1} \dots \int_{\gamma_N=0}^{2^{R_c-\phi(\gamma_1)-\phi(\gamma_2)-\dots-\phi(\gamma_{N-1})}-1} \frac{1}{\Gamma_1} \left(1 - \frac{\gamma_1}{\Gamma_1}\right) \frac{1}{\Gamma_2} \left(1 - \frac{\gamma_2}{\Gamma_2}\right) \dots \frac{1}{\Gamma_N} \left(1 - \frac{\gamma_N}{\Gamma_N}\right) d\gamma_N \dots d\gamma_2 d\gamma_1 \quad (29b)$$

$$\approx \frac{1}{\Gamma_1 \Gamma_2 \dots \Gamma_N} \int_{\gamma_1=0}^{2^{R_c}-1} \int_{\gamma_2=0}^{2^{R_c-\phi(\gamma_1)}-1} \dots \int_{\gamma_N=0}^{2^{R_c-\phi(\gamma_1)-\phi(\gamma_2)-\dots-\phi(\gamma_{N-1})}-1} d\gamma_N \dots d\gamma_2 d\gamma_1 \quad (29c)$$

$$= \frac{A_N(R_c)}{\Gamma_1 \Gamma_2 \dots \Gamma_N}. \quad (29d)$$

The steps are justified as follows: (29a) is the substitution of the pdf  $f(\gamma_i)$  given in (2) into (9e); (29b) MacLaurin series for exponential function  $\exp(-x_i) \approx 1 - x_i$  for  $x_i \rightarrow 0$ , (29c) expanding the resulting product as  $\prod_i (1 - x_i) \approx 1$  for  $x_i \rightarrow 0$ ; (29d) is proven in Lemma 5 and the assumption that the received SNRs are independently distributed, thus we can interchange the integral bounds.

**Lemma 5.** For any  $N \in \mathbb{N} \setminus \{1\}$ ,

$$A_N(x) = \int_{\gamma_N=0}^{2^x-1} \int_{\gamma_{N-1}=0}^{2^{x-\phi(\gamma_N)}-1} \dots \int_{\gamma_1=0}^{2^{x-\phi(\gamma_N)-\dots-\phi(\gamma_2)}-1} d\gamma_1 \dots d\gamma_{N-1} d\gamma_N \quad (30a)$$

$$= (-1)^N (1 - 2^x \cdot e_N(-x \ln(2))). \quad (30b)$$

Here,  $e_N(y) = \sum_{n=0}^{N-1} \frac{y^n}{n!}$  is the exponential sum function.

*Proof. Base case:* If  $N = 2$ , then (30a) is

$$A_2(x) = \int_{\gamma_2=0}^{2^x-1} \int_{\gamma_1=0}^{2^{x-\phi(\gamma_2)}-1} 1 d\gamma_1 d\gamma_2 = \int_{\gamma_2=0}^{2^x-1} \left[ \frac{2^x}{1+\gamma_2} - 1 \right] d\gamma_2 = 2^x (x \cdot \ln(2) - 1) + 1, \quad (31a)$$

which is (30b) for  $N = 2$ . So, the theorem holds for  $N = 2$ .

*Inductive hypothesis:* Suppose the theorem holds for all values of  $N$  up to some  $K \geq 2$ .

*Inductive step:* Let  $N = K + 1$ , then (30a) is

$$A_{K+1}(x) = \int_{\gamma_{K+1}=0}^{2^x-1} \underbrace{\int_{\gamma_K=0}^{2^{x-\phi(\gamma_{K+1})}-1} \dots \int_{\gamma_1=0}^{2^{x-\phi(\gamma_{K+1})-\dots-\phi(\gamma_2)}-1} 1 d\gamma_1 \dots d\gamma_K d\gamma_{K+1}}_{A_K(x-\phi(\gamma_{K+1}))} \quad (32a)$$

$$= \int_{\gamma_{K+1}=0}^{2^x-1} \left[ (-1)^K + \frac{2^x}{1+\gamma_{K+1}} \sum_{n=0}^{K-1} (-1)^{K+n+1} \frac{1}{n!} (x - \phi(\gamma_{K+1}))^n (\ln(2))^n \right] d\gamma_{K+1} \quad (32b)$$

$$= \int_{\gamma_{K+1}=0}^{2^x-1} \left[ (-1)^K + \frac{2^x}{1+\gamma_{K+1}} \sum_{n=0}^{K-1} (-1)^{K+n+1} \frac{1}{n!} (\ln(2))^n \times \sum_{k=0}^n (-1)^k \binom{n}{k} x^{n-k} \phi(\gamma_{K+1})^k \right] d\gamma_{K+1} \quad (32c)$$

$$= (-1)^K \gamma_{K+1} + 2^x \sum_{n=0}^{K-1} (-1)^{K+n+1} \frac{1}{n!} (\ln(2))^n \times \sum_{k=0}^n (-1)^k \binom{n}{k} x^{n-k} \frac{(\ln(1+\gamma_{K+1}))^{k+1}}{(k+1)(\ln(2))^k} \Big|_{\gamma_{K+1}=0}^{2^x-1} \quad (32d)$$

$$= (-1)^K \left( 2^x - 1 - 2^x \sum_{n=0}^{K-1} (-1)^n \frac{1}{n!} x^{n+1} (\ln(2))^{n+1} \underbrace{\sum_{k=0}^n (-1)^k \binom{n}{k} \frac{1}{k+1}}_{1/(n+1)} \right) \quad (32e)$$

$$= (-1)^{K+1} (1 - 2^x \cdot e_{K+1}(-x \ln(2))). \quad (32f)$$

The steps are justified as follows: (32b) is our inductive hypothesis; for (32c) we have used the binomial formula; (32f) we have used the following

$$\sum_{k=0}^n (-1)^k \binom{n}{k} \frac{1}{k+1} = \frac{1}{n+1} \sum_{k=0}^n (-1)^k \binom{n+1}{k+1} \quad (33a)$$

$$= \frac{-1}{n+1} \left[ \underbrace{\sum_{k=1}^{n+1} (-1)^k \binom{n+1}{k} + \binom{n+1}{0}}_{\sum_{k=0}^{n+1} (-1)^k \binom{n+1}{k} = (1-1)^{n+1} = 0} - \binom{n+1}{0} \right] = \frac{1}{n+1} \quad (33b)$$

and carried out some algebraic manipulations. Equation (32f) corresponds to (30b) for  $N = K + 1$ . So, the theorem holds for  $N = K + 1$ . Hence, by the principle of mathematical induction, the theorem holds for all  $N \in \mathbb{N} \setminus \{1\}$ .  $\square$

## APPENDIX B

### LEMMA 6

**Lemma 6.** For any  $N \in \mathbb{N} \setminus \{1\}$  and  $x > 0$ ,

$$X_N(x) = (A_1(x))^N > N! \cdot A_N(x) = Y_N(x), \quad (34)$$

where  $A_N(x)$  is given in Lemma 5.

*Proof.* For  $x = 0$  we have  $X_N(0) = 0$  and  $Y_N(0) = 0$  in (34). Next, show that the slope of  $X_N(x)$  is larger than the slope of  $Y_N(x)$  for  $x > 0$  and thus  $X_N(x) > Y_N(x)$ ,  $x \geq 0, \forall N$ .

$$\frac{d}{dx} X_N(x) = \frac{d}{dx} \left[ (2^x - 1)^N \right] = N 2^x \ln(2) (2^x - 1)^{N-1}, \quad (35a)$$

$$\frac{d}{dx} Y_N(x) = \frac{d}{dx} \left[ N! (-1)^N \left( 1 - 2^x \sum_{n=0}^{N-1} \frac{1}{n!} (-x \ln(2))^n \right) \right] \quad (35b)$$

$$= N! \ln(2) 2^x (-1)^{N+1} \left( \sum_{n=0}^{N-1} (-1)^n \frac{1}{n!} (x \ln(2))^n + \underbrace{\sum_{n=1}^{N-1} (-1)^n \frac{1}{(n-1)!} (x \ln(2))^{n-1}}_{-\sum_{n=0}^{N-2} (-1)^n \frac{1}{n!} (x \ln(2))^n} \right) \quad (35c)$$

$$= N! \ln(2) 2^x (-1)^{2N} \frac{1}{(N-1)!} (x \ln(2))^{N-1} = N 2^x \ln(2) (x \ln(2))^{N-1}. \quad (35d)$$

We have to show that

$$(2^x - 1)^{N-1} > (x \ln(2))^{N-1} \quad \text{for } x > 0. \quad (35e)$$

Since both sides in (35e) are equal for  $x = 0$  and have the same exponent, it is sufficient to show

$$\frac{d}{dx} (2^x - 1) > \frac{d}{dx} (x \ln(2)) \quad (35f)$$

$$\ln(2) 2^x > \ln(2). \quad (35g)$$

(35g) hold for  $x > 0$ . This completes the proof.  $\square$

## APPENDIX C

### PROOF OF THEOREM 4

Based on the outage probability analysis considered before the diversity gains for JD, MSC, and MRC are given by

$$d_{\text{JD}}(r) = - \lim_{\bar{\Gamma} \rightarrow \infty} \frac{\text{ld}(A_N(r, \bar{\Gamma})) - N \text{ld}(\bar{\Gamma})}{\text{ld}(N\bar{\Gamma})} \quad (36a)$$

$$= - \lim_{\bar{\Gamma} \rightarrow \infty} \left( r \frac{\text{ld}(N\bar{\Gamma})}{\text{ld}(N\bar{\Gamma})} + \frac{\text{ld}\left(\frac{1}{(N-1)!} (r \text{ld}(N\bar{\Gamma}))^{(N-1)} (\ln(2))^{(N-1)}\right)}{\text{ld}(N\bar{\Gamma})} - \frac{N \text{ld}(\bar{\Gamma})}{\text{ld}(N\bar{\Gamma})} \right) \quad (36b)$$

$$= N - r, \quad (36c)$$

$$d_{\text{MSC}}(r) = - \lim_{\bar{\Gamma} \rightarrow \infty} \frac{N \text{ld}(A_1(r, \bar{\Gamma})) - N \text{ld}(\bar{\Gamma})}{\text{ld}(N\bar{\Gamma})} \quad (36d)$$

$$= -N \lim_{\bar{\Gamma} \rightarrow \infty} \left( r \frac{\text{ld}(\bar{\Gamma})}{\text{ld}(N\bar{\Gamma})} - \frac{\text{ld}(\bar{\Gamma})}{\text{ld}(N\bar{\Gamma})} \right) \quad (36e)$$

$$= N \cdot (1 - r), \quad \text{and} \quad (36f)$$

$$d_{\text{MRC}}(r) = - \lim_{\bar{\Gamma} \rightarrow \infty} \frac{N \text{ld}(A_1(r, \bar{\Gamma})) - \text{ld}(N!) - N \text{ld}(\bar{\Gamma})}{\text{ld}(N\bar{\Gamma})} \quad (36g)$$

$$= -N \lim_{\bar{\Gamma} \rightarrow \infty} \left( r \frac{\text{ld}(\bar{\Gamma})}{\text{ld}(N\bar{\Gamma})} - \frac{\text{ld}(N!)}{N \text{ld}(N\bar{\Gamma})} - \frac{\text{ld}(\bar{\Gamma})}{\text{ld}(N\bar{\Gamma})} \right) \quad (36h)$$

$$= N \cdot (1 - r), \quad (36i)$$

respectively. The steps can be justified as follows: (36a), (36d), and (36g) is given by substituting (10b), (13), (17) into (23); in (36b) we use the infinite SNR properties of  $A_N(r, \bar{\Gamma})$  in (37c) and some algebraic manipulations; for infinite SNR the properties (38a) hold which yields (36c); in (36e) and (36h) we use the infinite SNR property of  $A_1(r, \bar{\Gamma})$  in (37a) and some algebraic manipulations; for infinite SNR the properties in (38a) hold which yields (36f) and (36i).

Substituting (22) into (10c) the constants  $A_N(r, \bar{\Gamma})$  and its special case  $A_1(r, \bar{\Gamma})$  can be given depending on the multiplexing gain  $r$  by

$$\lim_{\bar{\Gamma} \rightarrow \infty} A_1(r, \bar{\Gamma}) = \lim_{\bar{\Gamma} \rightarrow \infty} (2^{r \text{ld}(\bar{\Gamma})} - 1) = \lim_{\bar{\Gamma} \rightarrow \infty} 2^{r \text{ld}(\bar{\Gamma})}, \quad (37a)$$

$$\lim_{\bar{\Gamma} \rightarrow \infty} A_N(r, \bar{\Gamma}) = \lim_{\bar{\Gamma} \rightarrow \infty} \left( (-1)^N + 2^{r \text{ld}(N\bar{\Gamma})} \sum_{n=0}^{N-1} (-1)^{N+n+1} \frac{1}{n!} (r \text{ld}(N\bar{\Gamma}))^n (\ln(2))^n \right) \quad (37b)$$

$$= \lim_{\bar{\Gamma} \rightarrow \infty} 2^{r \text{ld}(N\bar{\Gamma})} \frac{1}{(N-1)!} (r \text{ld}(N\bar{\Gamma}))^{(N-1)} (\ln(2))^{(N-1)}, \quad (37c)$$

where (37c) can be justified with the infinite SNR properties in (38b). Further properties for infinite SNR are:

$$\lim_{\bar{\Gamma} \rightarrow \infty} \frac{\text{ld}(\bar{\Gamma})}{\text{ld}(N\bar{\Gamma})} = 1, \quad \lim_{\bar{\Gamma} \rightarrow \infty} \frac{(N-1) \text{ld}(\text{ld}(N\bar{\Gamma}))}{\text{ld}(N\bar{\Gamma})} = 0, \quad \lim_{\bar{\Gamma} \rightarrow \infty} \frac{\text{ld}(N!)}{N \text{ld}(N\bar{\Gamma})} = 0, \quad (38a)$$

$$\lim_{\bar{\Gamma} \rightarrow \infty} (\text{ld}(N\bar{\Gamma}))^{(N-1)} \gg \lim_{\bar{\Gamma} \rightarrow \infty} (\text{ld}(N\bar{\Gamma}))^{(N-n)} \quad \text{for } n = 2, \dots, N. \quad (38b)$$

This completes the proof.

## REFERENCES

- [1] A. Wolf, P. Schulz, D. Öhmann, M. Dörpinghaus, and G. Fettweis, "On the gain of joint decoding for multi-connectivity," in *Proc. IEEE Globecom (GC) (accepted for publication)*, Singapore, Dec. 2017.
- [2] A. Wolf, M. Dörpinghaus, and G. Fettweis, "Diversity-multiplexing tradeoff for multi-connectivity," in *Proc. IEEE International Conference on Communications (ICC) (will be submitted)*, Kansas City, MO, USA, May 2018.
- [3] P. Schulz, M. Matthe, H. Klessig, M. Simsek, G. Fettweis, J. Ansari, S. A. Ashraf, B. Almeroth, J. Voigt, I. Riedel, A. Puschmann, A. Mitschele-Thiel, M. Muller, T. Elste, and M. Windisch, "Latency critical IoT applications in 5G: Perspective on the design of radio interface and network architecture," *IEEE Communications Magazine*, vol. 55, no. 2, pp. 70–78, Feb. 2017.
- [4] D. Öhmann, "High reliability in wireless networks through multi-connectivity," Ph.D. dissertation, TU Dresden, Germany, 2017.
- [5] M. Eriksson, "Dynamic single frequency networks," *IEEE Journal on Selected Areas in Communications*, vol. 19, no. 10, pp. 1905–1914, Oct. 2001.
- [6] P. Marsch and G. P. Fettweis, *Coordinated Multi-Point in Mobile Communications: from Theory to Practice*. Cambridge University Press, 2011.
- [7] 3GPP, "Coordinated multi-point operation for LTE physical layer aspects," TR 36.819 V11.1.0, 2011.
- [8] A. Ravanshid, P. Rost, D. S. Michalopoulos, V. V. Phan, H. Bakker, D. Aziz, S. Tayade, H. D. Schotten, S. Wong, and O. Holland, "Multi-connectivity functional architectures in 5G," in *Proc. IEEE International Conference on Communications Workshops (ICCW)*, Kuala Lumpur, Malaysia, May 2016, pp. 187–192.
- [9] D. S. Michalopoulos, I. Viering, and L. Du, "User-plane multi-connectivity aspects in 5G," in *Proc. IEEE 23rd International Conference on Telecommunications (ICT)*, Thessaloniki, Greece, May 2016, pp. 1–5.
- [10] G. Pocovi, B. Soret, M. Lauridsen, K. I. Pedersen, and P. Mogensen, "Signal quality outage analysis for ultra-reliable communications in cellular networks," in *Proc. IEEE Globecom Workshops (GCW)*, San Diego, USA, Dec. 2015, pp. 1–6.
- [11] F. B. Tesema, A. Awada, I. Viering, M. Simsek, and G. P. Fettweis, "Mobility modeling and performance evaluation of multi-connectivity in 5G intra-frequency networks," in *Proc. IEEE Globecom Workshops (GCW)*, San Diego, USA, Dec. 2015, pp. 1–6.
- [12] J. J. Nielsen and P. Popovski, "Latency analysis of systems with multiple interfaces for ultra-reliable M2M communication," in *Proc. IEEE 17th International Workshop on Signal Processing Advances in Wireless Communications (SPAWC)*, Edinburgh, UK, Jul. 2016, pp. 1–6.
- [13] A. F. Molisch, *Wireless Communications*. John Wiley & Sons, 2012.
- [14] D. N. C. Tse, P. Viswanath, and L. Zheng, "Diversity-multiplexing tradeoff in multiple-access channels," *IEEE Trans. Inf. Theory*, vol. 50, no. 9, pp. 1859–1874, Sep. 2004.
- [15] E. Biglieri, R. Calderbank, A. Constantinides, A. Goldsmith, A. Paulraj, and H. V. Poor, *MIMO Wireless Communications*. Cambridge university press, 2007.
- [16] D. Slepian and J. Wolf, "Noiseless coding of correlated information sources," *IEEE Trans. Inf. Theory*, vol. 19, no. 4, pp. 471–480, Jul. 1973.
- [17] K. Anwar and T. Matsumoto, "Accumulator-assisted distributed turbo codes for relay systems exploiting source-relay correlation," *IEEE Commun. Lett.*, vol. 16, no. 7, pp. 1114–1117, Jul. 2012.
- [18] J. Garcia-Frias, "Joint source-channel decoding of correlated sources over noisy channels," in *Proc. IEEE Data Compression Conference (DCC)*, Snowbird, Utah, USA, May 2001, pp. 283–292.
- [19] M. C. Valenti and B. Zhao, "Distributed turbo codes: towards the capacity of the relay channel," in *Proc. IEEE Vehicular Technology Conference (VTC)*, Las Vegas, NV, USA, Sep. 2003, pp. 322–326.
- [20] M. Cheng, K. Anwar, and T. Matsumoto, "Outage probability of a relay strategy allowing intra-link errors utilizing Slepian-Wolf theorem," *EURASIP J. Adv. Signal Process.*, vol. 2013, no. 1, pp. 1–12, Feb. 2013.
- [21] X. Zhou, M. Cheng, X. He, and T. Matsumoto, "Exact and approximated outage probability analyses for decode-and-forward relaying system allowing intra-link errors," *IEEE Trans. Wireless Commun.*, vol. 13, no. 12, pp. 7062–7071, Dec. 2014.
- [22] A. El Gamal and Y.-H. Kim, *Network Information Theory*. Cambridge: Cambridge University Press, 2011.

- [23] A. Wolf, D. C. González, M. Dörpinghaus, L. L. Mendes, J. C. S. Santos Filho, and G. Fettweis, "Outage analysis for decode-and-forward multirelay systems allowing intra-link errors," *accepted for publication in IEEE Wireless Commun. Lett.*
- [24] D. C. González, A. Wolf, L. L. Mendes, J. C. S. Santos Filho, and G. Fettweis, "An efficient power allocation scheme for multirelay systems with lossy intra-links," *IEEE Trans. Commun.*, vol. 65, no. 4, pp. 1549–1560, Apr. 2017.
- [25] L. Zheng and D. N. C. Tse, "Diversity and multiplexing: a fundamental tradeoff in multiple-antenna channels," *IEEE Trans. Inf. Theory*, vol. 49, no. 5, pp. 1073–1096, May 2003.
- [26] D. Tse and P. Viswanath, *Fundamentals of Wireless Communication*. Cambridge University Press, 2005.
- [27] A. Goldsmith, *Wireless Communications*. Cambridge University Press, 2005.
- [28] B. Van Laethem, F. Quitin, F. Bellens, C. Oestges, and P. De Doncker, "Correlation for multi-frequency propagation in urban environments," *Progress In Electromagnetics Research Letters*, vol. 29, pp. 151–156, 2012.
- [29] T. Cover, "A proof of the data compression theorem of Slepian and Wolf for ergodic sources (corresp.)," *IEEE Trans. Inf. Theory*, vol. 21, no. 2, pp. 226–228, Mar. 1975.
- [30] T. M. Duman and A. Ghayeb, *Coding for MIMO Communication Systems*. John Wiley & Sons, 2008.
- [31] Z. Chen, J. Yuan, and B. Vucetic, "Analysis of transmit antenna selection/maximal-ratio combining in Rayleigh fading channels," *IEEE Trans. Veh. Technol.*, vol. 54, no. 4, pp. 1312–1321, 2005.
- [32] T. M. Cover and J. A. Thomas, *Elements of information theory*, 2nd ed. Hoboken, NJ: Wiley-Interscience, 2006.
- [33] M. Grieger, "Uplink joint detection in a realistic macro cellular environment," Ph.D. dissertation, TU Dresden, Germany, 2014.